Predicting failure using conditioning on damage history: Demonstration on percolation and hierarchical fiber bundles

J. V. Andersen[1,2] and D. Sornette[2,3,*]

[1]*U.F.R. de Sciences Economiques, Gestion, Mathématiques et Informatique, CNRS UMR 7536 and Université Paris X-Nanterre, 92001 Nanterre Cedex, France*

[2]*Laboratoire de Physique de la Matière Condensée, CNRS UMR 6622 and Université de Nice-Sophia Antipolis, 06108 Nice Cedex 2, France*

[3]*Institute of Geophysics and Planetary Physics and Department of Earth and Space Sciences, University of California, Los Angeles, California 90095, USA*

(Received 18 August 2005; published 18 November 2005)

We formulate the problem of probabilistic predictions of global failure in the simplest possible model based on site percolation and on one of the simplest models of time-dependent rupture, a hierarchical fiber bundle model. We show that conditioning the predictions on the knowledge of the current degree of damage (occupancy density p or number and size of cracks) and on some information on the largest cluster improves significantly the prediction accuracy, in particular by allowing one to identify those realizations which have anomalously low or large clusters (cracks). We quantify the prediction gains using two measures, the relative specific information gain (which is the variation of entropy obtained by adding new information) and the root mean square of the prediction errors over a large ensemble of realizations. The bulk of our simulations have been obtained with the two-dimensional site percolation model on a lattice of size $L \times L = 20 \times 20$ and hold true for other lattice sizes. For the hierarchical fiber bundle model, conditioning the measures of damage on the information of the location and size of the largest crack extends significantly the critical region and the prediction skills. These examples illustrate how ongoing damage can be used as a revelation of both the realization-dependent preexisting heterogeneity and the damage scenario undertaken by each specific sample.

DOI: 10.1103/PhysRevE.72.056124 PACS number(s): 62.20.Mk, 61.43.−j, 91.30.Px

I. INTRODUCTION

Despite the large amount of experimental data and the considerable effort that has been undertaken by material scientists [1], there is no comprehensive understanding of rupture phenomena but only a partial classification in restricted and relatively simple situations. This lack of fundamental understanding is reflected in the absence of reliable prediction methods for rupture, based on a suitable monitoring of the stressed system. The difficulties stem from the complex interplay between heterogeneities and modes of damage and the possible existence of a hierarchy of characteristic scales (static and dynamic) [2].

Here, we exploit this complexity to propose a minimal procedure (minimal in the sense of no additional or extraneous hypothesis, but simple exploitation of available information) to extract an optimum failure prediction based on the knowledge of present survival state. We believe this procedure to be relevant to most failure phenomena.

The idea underlying this paper was inspired by the method of "reverse tracing of precursors" (RTP) introduced in Refs. [3,4] as a method of earthquake prediction based on seismicity patterns. In a nutshell, the RTP method consists first in delineating a spatial domain $\mathcal{S}(t)$ by using a space-time correlation analysis of past seismicity up to the present time t and then in constructing precursory diagnostics based on past seismicity restricted to this spatial domain $\mathcal{S}(t)$ (called chains in Refs. [3,4]). In Refs. [3,4], the precursory functions used to issue a prediction are based on previously documented seismic anomalies (see [5] and references therein) and will not be our concern. Rather, the question we are asking is, what could justify the innovation presented in Refs. [3,4] to constrain the construction of precursory diagnostics to some special spatial domains recognized from some spatiotemporal correlation analysis of past seismicity? Indeed, Refs. [3,4] do not provide an explanation on why their method should work and what could be its underlying physical mechanism(s), since their approach is based on the pragmatic mathematical pattern recognition method initiated long ago by Gelfand *et al.* [6]. Our paper is the first one in a series which shows how the idea behind RTP can be actually justified on physical grounds and used for improving previous prediction methods for earthquakes or material ruptures.

We first present the problem and explore its implications for the percolation model and then test the robustness of the results and extend them to a time-dependent hierarchical fiber bundle model.

II. FORMULATION OF THE PERCOLATION MODEL

As a first step, we propose to formulate the problem with perhaps the simplest model of heterogenous media undergoing a transition, the site percolation model [7–9]. By doing so, we aim at capturing the essence of the idea.

Consider a two-dimensional lattice of $L \times L$ sites which are initially empty. We then fill one by one the sites at ran-

*Electronic address: vitting@unice.fr, sornette@moho.ess.ucla.edu

dom positions and denote by p the corresponding fraction of occupied sites. Any given realization $\mathcal{C}_L$ will be characterized by some threshold $p_c(\mathcal{C}_L)$ at which the occupied sites form a cluster which barely percolates from one side of the system to its opposite side. It is known that, for $L\to\infty$, $p_c(\mathcal{C}_L)$ becomes independent of the specific realization of the system and converges to a unique number $p_c^\infty=0.592\,746\,0 \pm 0.000\,000\,5$ [10]. It is also well known that, for finite L, $p_c(\mathcal{C}_L)$ is a random number distributed according to a probability density function (PDF) $P(p_c)$ centered on a value shifted downwards from p_c^∞ by an amount and with a width which are both proportional to $1/L^{1/\nu}$, where $\nu=4/3$ is the universal exponent (in two dimensions) of the correlation length, defined, roughly speaking, as the typical size of the largest cluster. The shift and width of the PDF $P(p_c)$ are characteristic of the so-called finite-size scaling of the critical percolation transition [11].

For our purpose which is to relate with the prediction of a rupture or an earthquake, we interpret p as the running time, which is also the fraction of the lattice which is damaged. We thus envision the two-dimensional lattice as being progressively damaged at a rate of one site failing per unit time. The percolation threshold $p_c(\mathcal{C}_L)$ then corresponds to the time when there is a connected path of damaged sites running from one side to the other, such that the system is deconnected into at least two pieces, a diagnostic of rupture. Hence, the progressive filling of the sites in the percolation problem described above corresponds to the progressive damage of an initially pristine system.

Roux *et al.* [12] have shown that rupture is equivalent to percolation in the limit of very large disorder and, by extension, rupture processes can be considered as nothing but (complicated) correlated percolation problems [2,13]. Since, by definition, the addition of new sites in percolation model has no interaction, correlation, or memory of the past, the formulation of the idea inspired by the RTP method in this context necessarily reduces the scope of the approach. This is because the information present in real rupture and earthquake cases based on correlation and memory in the time domain has no bearing in the prediction of the percolation threshold $p_c(\mathcal{C}_L)$. In subsequent papers, we will investigate different examples of "correlated" percolation—namely, models of rupture—in which time-dependent precursors can be coupled with the spatial organization of damage. The hierarchical time-dependent fiber-bundle model analyzed in Sec. V provides a first example of this class of processes.

III. PREDICTIONS OF THE PERCOLATION THRESHOLD

A. Hierarchy of prediction levels

Suppose that a given realization in a system of size $L\times L$ is at the cumulative fraction p of damaged sites. What level of prediction is possible for its percolation threshold $p_c(\mathcal{C}_L)$? We now describe different levels of prediction of the percolation threshold based on increasing the available information.

(i) The first level of prediction is what we call the unconditional prediction, which amounts to not even use the knowledge that the system has the cumulative fraction p of damaged sites. It corresponds to the statistical distribution of $p_c(\mathcal{C}_L)$. This is the information available at the beginning of a simulation.

(ii) The second level of prediction is to use the fact that we want to predict $p_c(\mathcal{C}_L)$ conditioned on the fact that we know that the system has reached the cumulative fraction p of damaged sites. It is obvious that this improves on the first level: for instance, if, by luck, p happens to be already quite large [say larger than the average of $p_c(\mathcal{C}_L)$] and the system is still not percolating, then we know for sure that the value of $p_c(\mathcal{C}_L)$ for this system will be larger than p.

(iii) The third level of prediction incorporates additional information on how the damage over the pL^2 sites is organized. For instance, typical experiments of rupture have access to the spatial organization of acoustic emissions, which provide clues on the localization of damage. In this spirit, suppose that we can measure the fraction of damaged sites belonging to the largest cluster at p or the size along the horizontal and vertical directions of the largest cluster. Then, this should give us some additional information to improve on the prediction. Indeed, if we measure for two given realizations that the largest cluster has a horizontal size close to L in the first one and $L/2$ in the second one for a given p, we can guess that the first system will in general percolate sooner [for a smaller $p_c(\mathcal{C}_L)$] than the second system.

(iv) One can imagine many other levels of prediction using all kinds of additional information, such as the statistics of the clusters, their shape, positions, etc.

(v) The last ultimate level of prediction is to use all the information on the exact locations of all damaged sites and condition the prediction of $p_c(\mathcal{C}_L)$ on this knowledge.

In the following, we implement the first three levels of predictions and show that we obtain substantial gains at the third level. This is perhaps not surprising, but this provides a quantitative demonstration on how prediction can be improved by using information on the spatial organization of damage. Additionally, it tells us what are the limits of predictability, given each level of information.

B. First and second prediction levels

The first prediction level described in Sec. III A amounts to constructing the standard probability distribution function $P_L(p_c)$ of the percolation thresholds, shown by the circles in Fig. 1 for $L=20$. We have used 50×10^6 realizations to get a good statistics. Such distribution is the standard tool for the study of finite-size scaling [11]. For our purpose, it quantifies the range of predictions for the percolation thresholds $p_c(\mathcal{C}_L)$ in the form of a probabilistic forecast.

Crosses, dots, and squares show the second prediction level, corresponding to the PDF's $P_L(p_c|p)$ conditioned on those systems which have not percolated for a fixed occupation density $p=0.50, 0.53$ and $p=0.55$, respectively. Since for $L=20$, the unconditional PDF $P_L(p_c)$ is quite broad with as many as 40% of the realizations percolating with $p_c(\mathcal{C}_L)<0.55$, the condition that $p_c(\mathcal{C}_L)$ has to be larger than 0.55 transforms $P_L(p_c)$ into a significantly more peaked conditional PDF $P_L(p_c|p=0.55)$. In the language of the prediction

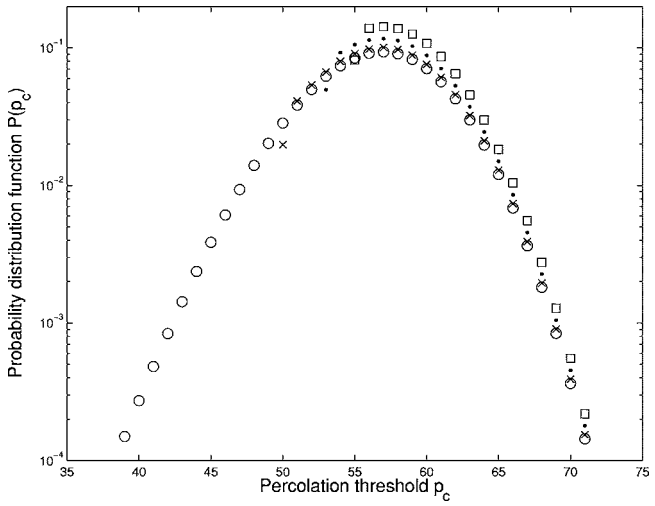

FIG. 1. Circles: standard probability distribution function (PDF) $P_L(p_c)$ as a function of the percolation threshold p_c (in percent) for $L=20$. Crosses: conditional PDF $P_L(p_c|p=0.5)$ conditioned on those systems which have not percolated for a fixed occupation density $p=0.5$. Dots: conditional PDF $P_L(p_c|p=0.53)$ conditioned on those systems which have not percolated for a fixed occupation density $p=0.53$. Squares: conditional PDF $P_L(p_c|p=0.55)$ conditioned on those systems which have not percolated for a fixed occupation density $p=0.55$.

problem, the PDF's $P_L(p_c|p)$ shown with the crosses, dots, and squares provide the probabilistic forecasts for rupture, available at "time" p and conditioned only on the knowledge of p.

C. Third prediction level

We implement the third prediction level described in Sec. III A in two ways. Let us call $p_\xi(p)$ the fraction of sites belonging to the largest cluster and $\xi(p)$ the largest of the linear size projected on the x and y axes of the largest cluster within the system when the occupancy density is p.

Figure 2 presents the PDF $P_L(p_c|p,p_\xi)$ conditioned on both p and $p_{\xi=6\%}$, for different values of p (crosses, $p=0.4$; dots, $p=0.45$; squares, $p=0.5$). For comparison, the unconditional distribution of the first prediction level is also shown with open circles. The gradual shift of the PDF $P_L(p_c|p,p_\xi)$ to larger values of p_c for increasing p shows that the measurement of the largest cluster size which is fixed for a given p in the percolating process makes it more likely to see percolation occurring at "late times" (i.e., for large p_c's) the larger the value of p. Intuitively, this just means that if one observes in two different systems for different values of p the *same* mass of the largest cluster, the system with the largest value of p is more likely to percolate at a later time. The shift and narrowing of the PDF's are clear illustration of the information one can gain by conditioning on relevant variables.

Figure 3 presents the PDF $P_L(p_c|p,\xi)$ conditioned on both p and $\xi=0.2L$ for different values of p (dots, $p=0.35$; squares, $p=0.4$). For comparison, the unconditional distribution of the first prediction level is also shown with open

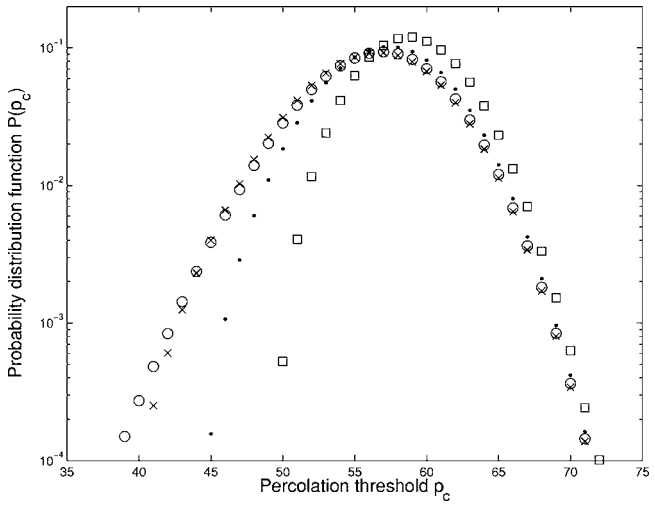

FIG. 2. PDF $P_L(p_c|p,p_\xi)$ as a function of p_c (in percent) conditioned on both p and $p_\xi=6\%$, where p_ξ is the fraction of sites belonging to the largest cluster, for different values of p (crosses, $p=0.4$; dots, $p=0.45$; squares, $p=0.5$). For comparison, the unconditional distribution of the first prediction level is also shown with open circles.

circles. The results are similar to those presented in Fig. 2, with a gradual shift and narrowing of the conditional PDF's to larger values of p_c for increasing p. Using the largest projected cluster should give even more information on the final value of p_c for a given system, since, e.g., two systems with the same p and p_ξ, but one having a more elongated largest cluster than the other, should help the former reach the percolation threshold sooner on average.

Figure 4 shows the PDF $P_L(p_c|p,\xi)$ for a fixed $p=40\%$ and different values of ξ: $\xi/L=0.04$ (crosses), $\xi/L=0.06$ (dots), $\xi/L=0.08$ (squares), and $\xi/L=0.1$ (triangles). The

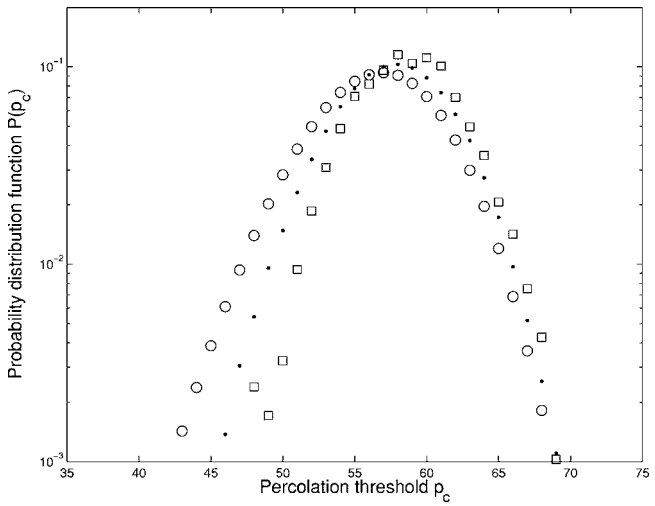

FIG. 3. PDF $P_L(p_c|p,\xi)$ as a function of p_c (in percent) conditioned on both p and $\xi=0.2L$, where ξ is the largest of the linear size projected on the x and y axes of the largest cluster within the system, for different values of p (dots, $p=0.35$; squares, $p=0.4$). For comparison, the unconditional distribution of the first prediction level is also shown with open circles.

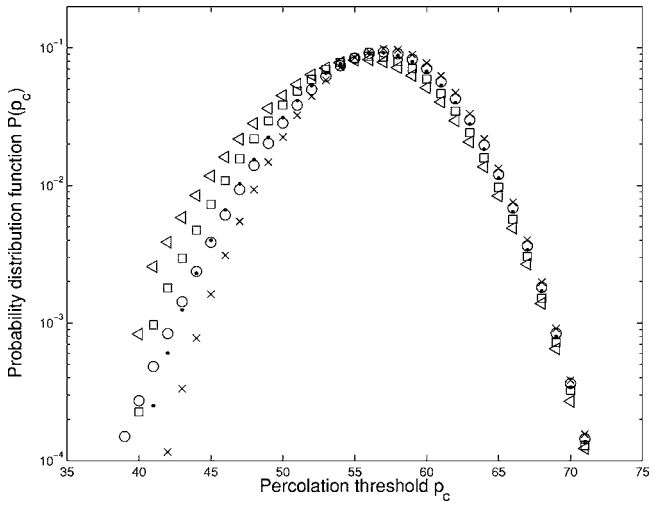

FIG. 4. Same as Fig. 3 for a fixed $p=40\%$ and different values of ξ: $\xi/L=0.04$ (crosses), $\xi/L=0.06$ (dots), $\xi/L=0.08$ (squares), and $\xi/L=0.1$ (triangles). The open circles represent the unconditional PDF $P_L(p_c)$ for reference.

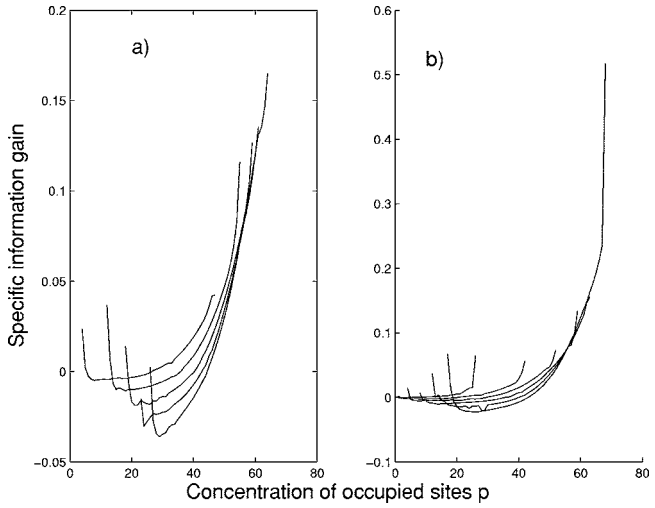

FIG. 5. Panel (a): relative specific information gain $I(p,p_\xi)$ as a function of p (in percent) for various values of $p_\xi = 2\%, 4\%, 6\%, 8\%, 10\%$ from left to right. Panel (b): relative specific information gain $I(p,\xi)$ as a function of p for various values of $\xi/L=10\%, 20\%, 30\%, 40\%, 50\%, 60\%$ from left to right.

open circles represent the unconditional PDF $P_L(p_c)$ for comparison.

IV. MEASURES OF GOODNESS OF THE THIRD LEVEL PREDICTIONS

A. Information gain

The standard measure of the improvement in the quality of forecasts when going from the first to the third prediction level is the information gain $H-H_{sc}$, where H is the unconditional entropy defined by

$$H = -\int P(p_c)\ln[P(p_c)]dp_c. \tag{1}$$

We consider two possible conditional entropies $H_{sc}(p,p_\xi)$ and $H_{sc}(p,\xi)$ associated with the two conditional schemes of the third level prediction discussed in the previous section:

$$H_{sc}(p,p_\xi \text{ or } \xi) = -\int P(p_c|p,p_\xi \text{ or } \xi)\ln[P(p_c|p,p_\xi \text{ or } \xi)]. \tag{2}$$

The relative "specific information gain" I $(p, p_\xi$ or $\xi)$ is then defined by

$$I(p,p_\xi \text{ or } \xi) \equiv \frac{1}{H}[H - H_{sc}(p,\ p_\xi,\ \text{or } \xi)]. \tag{3}$$

Figure 5 shows $I(p,p_\xi)$ [panel (a)] and $I(p,\xi)$ [panel (b)] as a function of p for various values of p_ξ and ξ. The relative specific information gains $I(p,p_\xi)$ and $I(p,\xi)$ have qualitatively the same behavior, characterized by three regimes.

(i) For small values of p (the smaller p_ξ or ξ, the smaller the values of p for which this regime holds), we observe some information gain when adding the information on p_ξ or ξ. This information gain can be ascribed to the realizations which initially (i.e., for small p) have an abnormal large value of p_ξ or ξ and therefore are likely to percolate before the typical behavior. Knowledge of these anomalously large p_ξ or ξ, when they occur, gives an improvement for the prediction of the percolation of these systems. Translated in the context of the prediction of rupture, the information gain shown in Fig. 5 for small p's is based on the detection of anomalous cracks or defects at an early stage. It is important to stress that the information gain is not uniform over all realizations: most realizations are not much more predictable by adding the information on p_ξ or ξ for small p's; only those which have anomalous defects can be better predicted. This result is reasonable and retrieves the standard approach in applications of mechanical engineering to the prediction of rupture in which the major efforts are put in the detection of possible initial flaws in the material or structure.

(ii) For intermediate values of p, the information gain obtained by conditioning on p_ξ or ξ is limited if not negative, since for these values of p the imposed p_ξ or ξ correspond to "normal" values.

(iii) Finally, for the larger p's, the information gain accelerates and become large since it becomes very unlikely to observe systems with such small values of p_ξ or ξ. Therefore, knowledge that a given realization has an anomalously small p_ξ or ξ provides highly meaningful information that percolation will require a much larger value of p than the current value.

While the relative specific information gains $I(p,p_\xi)$ and $I(p,\xi)$ have qualitatively the same behavior, the gain is much larger for the latter compared with the former: this is because the geometrical size of the larger cluster is much more relevant for percolation than the total number of sites in the large cluster.

B. rms of prediction errors

We now quantify the errors of the prediction of the realization specific percolation threshold $p_c(\mathcal{C}_L)$ based on the

conditioning on p and p_ξ or ξ. We imagine a situation mimicking a real-life situation in which one monitors the cumulative level of damage p of a sample as well as the largest crack in the system. Conditioned on the knowledge of p and p_ξ or ξ for a given realization, how well can we predict the rupture time $p_c(\mathcal{C}_L)$ of the sample?

In order to address this question, we have first made 50×10^6 realizations of system sizes $L=20$ to obtain a good estimate of the conditional distributions $P(p_c|p,p_\xi)$ and $P(p_c|p,\xi)$, which will be our prediction tools. Having sampled these conditional distributions, we then constructed additional realizations that we monitored to measure their $p_\xi(p)$ and $\xi(p)$ as a function of p. For a given realization at a given p, knowing the corresponding specific $p_\xi(p)$, our prediction is nothing but $P(p_c|p,p_\xi(p))$. Similarly, for a given realization at a given p, knowing the corresponding specific $\xi(p)$, our prediction is nothing but $P(p_c|p,\xi(p))$. Note that our forecasts are intrinsically probabilistic, by construction. However, each probabilistic forecast can be translated into a single predicted number $p_c^{\text{predicted}}(p)$—for instance, the median of $P(p_c|p,p_\xi(p))$ or $P(p_c|p,\xi(p))$—complemented with an uncertainty given by some measure of the width of these distributions (standard deviation or quantiles).

In order to assess the quality of such predictions, we need to construct statistics over ensembles of forecasts. In addition, we would like to study how the quality of the predictions evolves with the degree of damage p, in particular to test if we get advanced warning and how the prediction improves or deteriorates as a function of p. Since, for each p, we have two distributions of p_ξ and ξ which move with p, the amount of data to visualize is too large to remain comprehensible. We propose to focus on fixed quantiles q of the distributions of p_ξ and ξ—say, $q=5\%$ and $q=95\%$—so that we issue predictions based on the pairs $p,p_\xi^q(p)$ [and similarly $p,\xi^q(p)$] where $p_\xi^q(p)$ [$\xi^q(p)$] is the qth quantile of the distribution of p_ξ [ξ] for the cumulative damage p.

For such a prediction, we can assess its error by constructing the rms (root mean square) of errors:

$$Q(p) \equiv \langle [p_c^{\text{predicted}}(p) - p_c^{\text{true}}]^2 \rangle^{1/2}, \tag{4}$$

where p_c^{true} is the true value observed for the given system and where $p_c^{\text{predicted}}(p)$ is our predicted value of p_c for a given system and for a given p and using a given quantile q of the distribution of p_ξ (ξ^q) for the cumulative damage p. As our prediction $p_c^{\text{predicted}}(p)$ for p_c, we have used the median value of the conditional cumulative distribution defined by

$$P_{\leqslant}(p_c^{\text{predicted}}|p,\ p_\xi^q(p),\ \text{or}\ \xi^q(p)) = 1/2. \tag{5}$$

Figure 6 shows $Q(p,\xi)$ for $q=5\%$, $q=50\%$ and $q=95\%$, when using $P(p_c|p,\xi^q(p))$ as the predictor, as a function of p. The triangles correspond to $q=5\%$, the dots to $q=95\%$, and the crosses to $q=50\%$, while the circles show $Q(p)$ obtained using the conditioning only on p for comparison. The corresponding figure when using $P(p_c|p,p_\xi(p))$ as the predictor is very similar and is thus not shown. Figure 7 shows the gain in rms $Q(p)-Q(p,\xi)$ when adding the information on ξ. These figures show the result of an implementation which mimics a real experiment of a material progressively

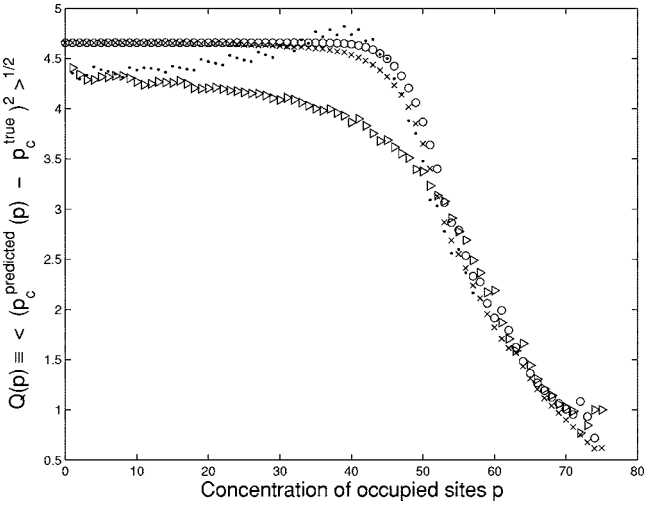

FIG. 6. rms $Q(p,p_\xi)$ (in percent) of the prediction errors defined by Eq. (4) with Eq. (5), for the quantiles $q=5\%$, $q=50\%$ and $q=95\%$ of the distribution of ξ at fixed p, when using $P(p_c|p,\xi^q(p))$ as the predictor, as a function of the damage parameter p (in percent). Triangle, $q=5\%$; dots, $q=95\%$; crosses, $q=50\%$; circles, $Q(p)$ obtained using the conditioning only on p. This rms $Q(p,p_\xi)$ should be compared with the standard deviation equal to 4.66% of the unconditional distribution of percolation thresholds, to illustrate the gain in prediction accuracy deriving from the added information.

brought to failure: one would for a given time (that is, p) measure the largest crack and, from the PDF's documented from earlier experiments, get an estimate of p_c corresponding to that p,ξ. Notice that all three estimates in Fig. 6 coincide for small p's. The reason is of course that the PDF's for small p are very close to each other, whether the conditioning is on ξ (corresponding to a small value of p) or just conditioned on p itself.

These figures confirm the signicant gain in prediction accuracy when conditioning the forecast on the $q=5\%$ and q

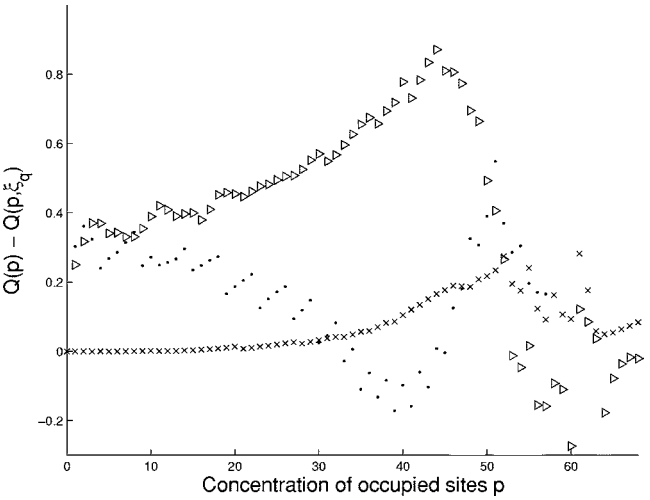

FIG. 7. Gain in rms $Q(p)-Q(p,\xi)$ when adding the information on ξ, where $Q(p,\xi)$ is shown as the triangles ($q=5\%$), dots ($q=95\%$), and crosses ($q=50\%$) and $Q(p)$ is shown in Fig. 6 with circles.

=95% quantiles of the distribution of ξ (p_ξ). The $q=5\%$ quantile selects those realizations such that their largest cluster is so small that 95% of the realizations have a bigger largest cluster. Conditioning on this information gives a significant gain in the forecast, especially for advanced warnings. The improvement deteriorates when p approaches the average percolation threshold and even changes sign with a worse quality for p larger than about 54%. We observe the opposite trend when conditioning on the $q=95\%$ quantile of the distribution of ξ, corresponding to those realizations which have an anomalously big largest cluster so that only 5% of the realizations have a bigger largest cluster. In this case, the prediction accuracy is improved above for $p > 0.45$.

V. HIERARCHICAL FIBER RUPTURE MODEL WITH TIME DEPENDENCE

The principles underlying the results on the percolation model presented above are of general validity. Our following papers will investigate their application and extension to other model systems and to different real systems including concrete engineering systems (material failure, structural collapse) and geophysical systems (earthquakes, landslides). However, it is worthwhile already to present preliminary results obtained on a more realistic (even still highly simplified) model of damage evolution and rupture, to illustrate our point.

A. Definition of the hierarchical bundle model

The model describes the time evolution of damage leading to the culminating global failure of a bundle of fibers in a creep experiment. The model has been studied in [14–16]. Consider a hierarchical bundle of elastic fibers subjected to a constant stress load σ per fiber applied at time $t=0$. The topology of the system is as follows. Each fiber is associated with another fiber in a pair. Then, two neighboring pairs are associated to each other, forming a pair of two pairs and so on iteratively up in a sequence of levels, thus defining a discrete hierarchical tree of local coordination 2. A system containing n such levels has 2^n fibers. This topology impacts the dynamics of fiber rupture in the following way. When one of the two fibers of a given pair fails, its stress load is transferred instantaneously to the surviving fiber, such that its load is doubled. When this fibers breaks, its load is transferred to the pair of fibers associated with it if this second pair is still present. Otherwise, it is transferred to the pair of two pairs linked at the next hierarchical level. The last ingredient of the model is to specify how a fiber fails under a given stress load history. Given some stress history $s(t'), t' \geqslant 0$, a fiber is assumed to break at some fixed random time, where the probability that this random time takes a specific value t is specified by its cumulative distribution function

$$P_0(t) \equiv \int_0^t p_0(t')dt' = 1 - \exp\left\{ - \kappa \int_0^t [\sigma(t')]^\rho \mathrm{d}t' \right\}. \quad (6)$$

This law captures the physics of stress corrosion and of failure due to stress-assisted thermal activation and progressive damage. A system of 2^n fibers is fully specified by attributing to each fiber $i=1,\ldots,2^n$ at the beginning of the experiment a fixed failure time t_i taken from the distribution (6). The failure time t_i is by definition the time at which the fiber i would have broken if the stress had stayed constant equal to the initial value σ. But the fibers are coupled through the hierarchical load transfer rule defined above. As a consequence of the hierarchical structure of the load transfers occurring at each rupture, the stress applied to a given fiber may increase, leading to a shortening of its lifetime.

Let us consider quantitatively the effect of the rupture of one fiber at time t_1 on the other fiber of its pair, which would have broken at time t_2 without this additional load transfer. For a population of such pairs of fibers, the distribution of the time-to-failure for the remaining fiber is obtained from Eq. (6) by taking the stress equal to σ up to t_1 and equal to 2σ from t_1 up to the second rupture, which now occurs at a time $t_{12} < t_2$ itself function of t_1 and t_2:

$$P_0(t_{12}) = 1 - \exp\{-\kappa\sigma^\rho[t_1 + 2^\rho(t_{12} - t_1)]\}. \quad (7)$$

Doing this calculation for the ensemble, the population of fibers must be the same since the population is homogeneous at this level and $P_0(t_{12})$ should therefore also be equal to $1-\exp(-\kappa\sigma^\rho t_2)$. Considering that t_{12} is a function of t_2 and identifying this expression with Eq. (7), we rederive the fundamental result [14] that the time-to-failure of a fiber is modified from its initial value t_2 to a smaller failure time t_{12} by the influence of the other fiber which has failed at the earlier time t_1, according to

$$t_{12} = t_1 + 2^{-\rho}(t_2 - t_1). \quad (8)$$

The inequality $2^{-\rho} \leqslant 1$ (for $\rho > 0$) ensures that $t_1 \leqslant t_{12} \leqslant t_2$. This corresponds to a genuine cooperative process as the time-of-failure of the second fiber is decreased by the load transfer from the first fiber. This remarkable result holds for any realization of the stochastic process. Let us stress that this result now applies not only at the level of individual fibers but at all levels within the hierarchy: if t_1 and t_2 are the lifetimes of two uncoupled bundles, then Eq. (8) describes the effect of the rupture of the first bundle on the second one which sees its load doubling at time t_1. The relation (8) forms the basis for analytical as well as numerical simulations. In particular, an exact Monte Carlo calculation of the probability distribution of failure times of this hierarchical system indicates that the distribution of failure times for the whole system is renormalized from $P_0(t)$ into a staircase (or jumps from 0 to 1) at a well-defined nonzero critical time t^*, as the system size n tends to infinity, according to a generalized central-limit theorem. It has also been shown theoretically and numerically that the rate of fiber failures diverges (up to finite-size effects) according to a power law $\sim 1/(t^* - t)^{p(\rho)}$ upon the approach to the global rupture time t^* for $\rho > 1$, where p depends on ρ [15,16]. In our investigation below, we take $\kappa=1$ and $\rho=2$.

B. Third level prediction by conditioning the distribution of lifetimes on the observation of the largest crack

We address the central question of this paper—namely, how the revelation of information up to the present in the

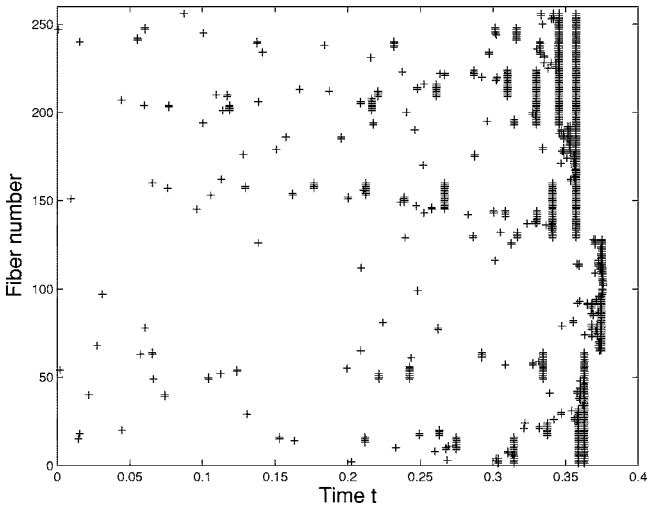

FIG. 8. A specific realization of the space-time evolution of fiber damage for a system of $2^8=256$ fibers. The fibers are numbered sequentially from 1 to 256 along the vertical axis. When a given fiber i breaks at some time t_i, a symbol + represents the spatial position and failure time of this event.

form of the partial knowledge of where and when fibers or groups of fibers have broken may be exploited to bracket better and better the realization-specific lifetime of a whole given system.

In order to mimic a real-life situation, we consider a creep experiment of our hierarchical fiber system such that, at time 0, a stress σ is applied. We have no access to the specific individual lifetimes of the individual constituting fibers, only to their PDF $p_0(x)$. At time passes, damage occurs—that is, fibers break—thus revealing their initial lifetimes. The situation becomes of course complicated because of the interactions between the fibers through the hierarchical stress load defining the model, as the damage spreads accross the levels of the hierarchy. In a real-life experiment, the damage would be measured, for instance, by acoustic emissions, with both time and space localization giving information on which fibers have been broken and at what time.

Our goal here is to construct schemes that uses some information in space and time on the damage that occurred until time t to form a better prediction for the rupture of the next level of the hierarchy and for the whole system, in the form of a PDF of lifetimes for the total system.

Figure 8 gives an illustration of the space-time evolution of fiber damage for a system of $2^8=256$ fibers. One can observe a transition from initial random uncorrelated ruptures to a progressive organization with growth of "cracks" and fusion between "cracks" associated with the acceleration of damage up to the culmination global failure.

Now, suppose that we observe the evolution of such a system from time 0 to some "present" time t, before complete failure. Furthermore, suppose that our measurement is imperfect and we do not have access to all the information on the position and times of individual fiber failures. Let us assume that we only know the size 2^m of the largest crack (or bundle) that has broken up to time t and some addition information on the fibers that broke within this crack at earlier

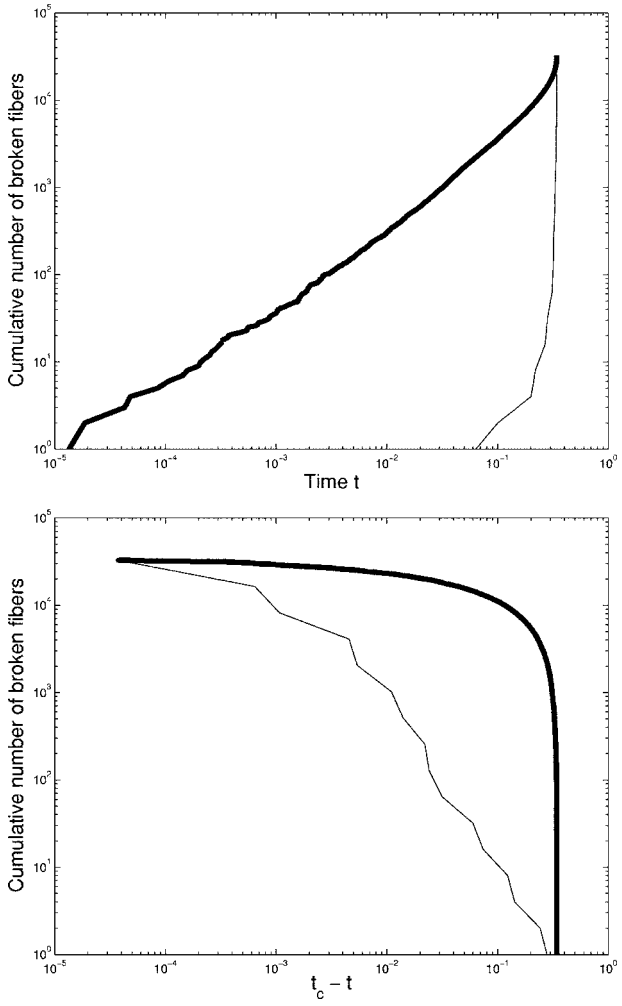

FIG. 9. (Top) Two different measures of the cumulative number of broken fibers as a function of time t for a given realization. The thick curve shows the unconditional cumulative number of broken fibers. The thin curve shows the (conditional) cumulative number of broken fibers, which broke either within the largest crack identified up to time t or within its complement in their pair within the hierarchy. (Bottom) This graph shows the same two curves in log-log scales with time t replaced by t_c-t, where t_c is the global time of failure (only known at the end). This log-log representation allows us to visualize the power-law acceleration characterizing the final critical regime before complete rupture, which is much more apparent in the conditional cumulative number of broken fibers.

times. Is this knowledge useful? Figure 9 shows two different measures of the cumulative number of broken fibers as a function of t (in log-log scales) for a given realization. The thick curve shows the unconditional cumulative number of broken fibers. The thin curve shows, as a function of time t, the cumulative number of broken fibers, which broke either within the largest crack or within its complement in their pair within the hierarchy. It is worth emphasizing that the time evolution of both cumulative damage is knowable at each time t. One can observe a striking difference, illustrating vividly the impact of conditioning on some available partial information on the ongoing damage, in order to improve the prediction of the global failure: in the absence of conditioning (we count all broken fibers), one can observe mostly a

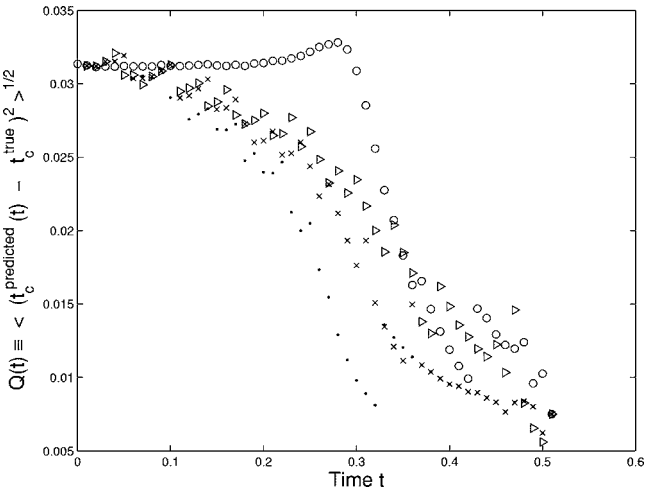

FIG. 10. Root mean square $Q(t)$ of the error or difference between predictions made at time t of the global rupture time and the true realized one as a function of time t for four distinct prediction schemes using different conditioning, similarly to Fig. 6 previously constructed for the percolation model. The system used here has 2^8 fibers and $\rho=2$. The ○ symbols correspond to a prediction at time t of the failure time t_c based solely on the information that the system has not yet broken. For the other curves, we constructed the distribution of failure times over 10^6 realizations for the different conditioning. The triangles correspond to the rms $Q(t)$ obtained by using the 5% quantile of the distribution of failure times over these 10^6 simulations. Specifically, for a given system and at a given time t, we measure the size ξ of the largest failed cluster and then read from the distribution of failure times for the same time t and same cluster size ξ the 5% quantile that we take as the prediction for the failure time. Similarly for the crosses and dots corresponding, respectively, to the 50% and 95% quantiles. Note that in our system of 2^8 fibers, there are eight possible sizes of "cracks" larger than 1—namely, 2,4,8,…,128,256. These curves are obtained by averaging over 10^5 realizations. These rms $Q(p)$ for the five prediction schemes should be compared with the standard deviation equal to 0.0311 of the unconditional distribution of failure times t_c, to illustrate the gain in prediction accuracy deriving from the added information obtained from conditioning.

linear increase and, only at the very end, can one see an acceleration [which is a power law of $1/(t_c-t)$ as shown in the inset]. In contrast, with the conditioning on the largest crack and its complement, the power-law regime is extended to very early time.

This result cannot be stressed sufficiently: in the past two decades, material failure of heterogeneous materials has been shown to belong to the class of dynamic critical phenomena (see, for instance, the review in [2] and references therein), but the critical region is in general difficult to observe and rather reduced in practical situations, thus hindering applications (this is why other techniques have been developed to enhance the predictability by extending the region over which critical information can be extracted [17,18]). What is remarkable in Fig. 9 is that focusing on the largest current crack and its neighborhood enhances the critical region tremendously, thus offering a large potential for prediction at early times.

Figure 10 is the equivalent for the hierarchical rupture model of Fig. 6 previously constructed for the percolation model. It shows the root mean square of the error or difference between predictions of the global rupture time and the true realized one, for four distinct prediction schemes using different conditioning. The improvement due to conditioning is qualitatively similar but quantitatily stronger than for the percolation model. This can be expected since the hierarchical bundle model has a dynamics in which the failure times of fibers keep the memory of past ruptures: the failure of a fiber is a function of all the previous ruptures that impacted the load history on this fiber. In constrast, the rupture of a bond in the percolation model is absolutely independent of past damage (except for the fact that the rupture occurs on remaining intact bonds, which is the mechanism underlying the benefits of conditioning exploited in previous sections). The existence of memory is expected, and one can verify that it improves the prediction performance: we conjecture more generally that the larger the connectivity and interactions between elements, the better should be the improvement of prediction quality with conditioning upon new information.

VI. CONCLUDING REMARKS

Our goal has been to demonstrate that one can predict the percolation or rupture threshold, based on knowledge of the amount of the current damage and on some information on the largest cluster or crack in the system. This problem was inspired by the idea of constructing better predictors for earthquakes and ruptures based on a combination of the space and time organization of damage. In this paper, which is the first of a series, we have first considered perhaps the worst and most difficult case for prediction—namely, percolation—because in this model damage has no memory of the past and no space-time correlation exists other than the properties associated with the geometry of connectivity. Similar results, not shown here, have been obtained for other lattice sizes $L=10$ and $L=30$, 40, and 50.

Then, we have illustrated the robustness of the results presented for the percolation model on one of the simplest model of time-dependent rupture, a hierarchical fiber bundle model. We have shown that conditioning the measures of damage on the information of the location and size of the largest crack extends significantly the critical region and the prediction skills.

We will show in subsequent papers that the predictions obtained in more realistic models of rupture which include realistic correlation in the space-time organization of damage and of cracks are significantly better, still. But our goal has been reached here by showing that, in the worst possible and most difficult case for prediction, we can achieve significant gains by implementing the conditioning of some information on the spatial organization of damage. In our practical implementation, we have considered the simplest information and many other algorithms can be developed to improve on our results. This will be developed in future papers.

ACKNOWLEDGMENTS

We are grateful to V. Keilis-Borok and I. Zaliapin for stimulating discussions.

[1] *Fracture*, edited by H. Liebowitz (Academic Press, New York, 1984), Vols. I–VII.
[2] D. Sornette, in *Handbook of Materials Modeling*, edited by S. Yip (Springer Science and Business Media, Berlin, 2005), Vol. I, pp. 1313–1331.
[3] P. Shebalin, V. Keilis-Borok, I. Zaliapin, S. Uyeda, T. Nagao, and N. Tsybin, Earth, Planets Space **56**, 715 (2004).
[4] V. Keilis-Borok, P. Shebalin, A. Gabrielov, and D. Turcotte, Phys. Earth Planet. Inter. **145**, 75 (2004).
[5] V. I. Keilis-Borok and A. Soloviev, *Nonlinear Dynamics of the Lithosphere and Earthquake Prediction* (Springer-Verlag, Berlin, 2003).
[6] I. M. Gelfand, Sh. A. Guberman, V. I. Keilis-Borok, L. Knopoff, F. Press, E. Ya. Ranzman, I. M. Rotwain, and A. M. Sadovsky, Phys. Earth Planet. Inter. **11**, 227 (1976).
[7] Percolation Structures and Processes, edited by G. Deutscher, R. Zallen, and J. Adler (The Israel Physical Society, Bristol, 1983).
[8] G. Grimmett, *Percolation* (Springer, New York, 1989).
[9] D. Stauffer and A. Aharony, *Introduction to Percolation Theory*, 2nd ed. (Taylor & Francis, London, 1994).
[10] R. M. Ziff, Phys. Rev. Lett. **69**, 2670 (1992).
[11] C.-K. Hu, J. Phys. A **27**, L813 (1994).
[12] S. Roux, A. Hansen, H. Herrmann, and E. Guyon, J. Stat. Phys. **52**, 237 (1988).
[13] D. Sornette, *Critical Phenomena in Natural Sciences (Chaos, Fractals, Self-organization and Disorder: Concepts and Tools)*, 2nd ed., Springer Series in Synergetics (Springer-Verlag, Heidelberg, 2004).
[14] W. I. Newman, A. Gabrielov, T. Durand, S. L. Phoenix, and D. Turcotte, Physica D **77**, 200 (1994).
[15] W. I. Newman, D. L. Turcotte, and A. M. Gabrielov, Phys. Rev. E **52**, 4827 (1995).
[16] H. Saleur, C. G. Sammis, and D. Sornette, J. Geophys. Res. **101**, 17661 (1996).
[17] A. Johansen and D. Sornette, Eur. Phys. J. B **18**, 163 (2000).
[18] D. Sornette, Proc. Natl. Acad. Sci. U.S.A. **99**, Suppl. 1, 2522 (2002).